PHYSICS TODAY

MAY 1993

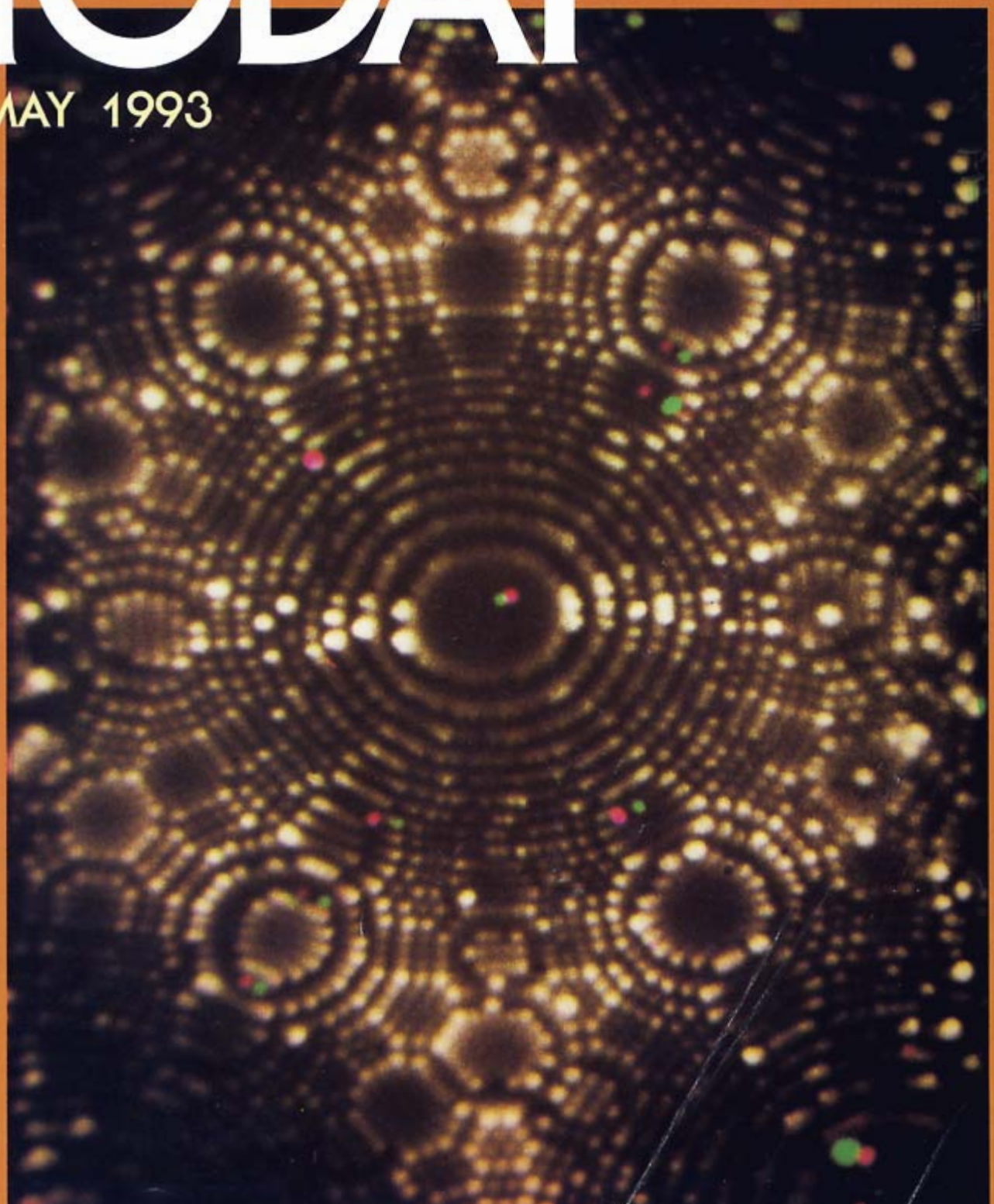

ATOM-PROBE FIELD ION MICROSCOPY

A technique first used for imaging atoms now permits the study of mechanisms and energetics of atomic processes on solid surfaces and the single-atom and atomic-layer chemical analysis of surfaces.

Tien T. Tsong

Scientists are always pushing to new frontiers, which often involve questions about phenomena that occur on very large or very small scales. Astronomers search for new stars millions of light-years away in a quest to learn how these stars and the universe were born, and particle physicists look at elementary particles of size less than 10^{-17} cm in an effort to understand fundamental interactions. Meanwhile, however, many biologists, chemists and condensed matter physicists are trying to understand natural phenomena that we encounter every day and that occur on some intermediate scale. Questions at this scale are posed in terms of interactions between electrons or atoms and chemical bonds or in terms of atomic theories. The motivation is not only scientific curiosity but also a desire to discover new effects, create new molecules and materials, and develop new technologies that may benefit society. Although a single interaction, electromagnetism, determines the chemical and physical properties of molecules and materials, nature manifests electromagnetic forces in so many forms and in so many phenomena that many of them are by no means understood. One of the powerful tools at our disposal for studies on the microscopic scale or atomic scale is the atomic-resolution microscope.

Microscopy can be traced back as far as the mid-15th century, before Galileo. However, not until the 1950s, when Erwin W. Müller invented the field ion microscope, did anyone succeed in seeing atoms as the building blocks of a solid.[1] But "seeing" is only one important aspect of atomic-resolution microscopy. Others include the elemental identification of atoms in a sample and the determination of the physical and chemical properties, such as the binding energy and electronic density of states, of each of these atoms in its own site. In the late 1960s Müller conceived the idea of making an atom-probe FIM by combining a field ion microscope and a mass spectrometer with single-ion detection sensitivity. He and his coworkers successfully developed a prototype and showed that single-atom chemical analysis of a material was possible.[2]

Tien Tsong is a Distinguished Professor at Pennsylvania State University, in University Park, and a Distinguished Research Fellow and director of the Institute of Physics at the Academia Sinica, in Taipei, Taiwan. He is currently on leave from the former position.

Atom-probe field ion microscopy, while restricted in its choice of samples to sharp tips having a radius in the range of 100–1200 Å, has become useful in studies of the dynamical behavior and energetics of atoms on metal surfaces and in atomic-layer chemical analysis of alloy surfaces in surface segregation. It can also be used to study the effects of high electric fields on surface atoms, which can lead to applications in atomic manipulation.

Imaging atoms is no longer a monopoly of the field ion microscope. Electron microscopes and scanning tip microscopes, which include the scanning tunneling microscope and the atomic force microscope, have now also achieved this goal. Because these microscopes impose less stringent requirements on both the materials studied and on their geometries, and because they can be operated in a wider range of magnifications and resolution than can the FIM, they are finding a wider range of applications. Single-atom chemical analysis, however, is still unique to atom-probe field ion microscopy.

As the structural features of advanced materials get smaller and smaller, they are getting closer in size to, or even becoming smaller than, the field ion tips. When the samples get smaller, the surface-to-volume ratio gets bigger and therefore the effects of the surface become more important. Also, many effects of the high electric field (on the order of a volt per angstrom) found and studied on the emitter surfaces are finding application in electron and ion sources the size of single atoms, in liquid metal ion sources and in the manipulation of atoms by field evaporation and field-gradient-induced surface diffusion. Thus the atom-probe field ion microscope is gradually being recognized as a research tool of considerable power. In this article I briefly review recent developments in atom-probe field ion microscopy and describe the tool's application to the study of the dynamical behavior and energetics of atoms on metal surfaces and to the atomic-scale chemical analysis of alloy surfaces. (Other reviews have covered applications to metallurgy, materials science and liquid metal ion sources.[3])

The microscope

An atom-probe field ion microscope is both a field ion microscope and a mass spectrometer.[4] The sample is a field emitter tip, usually prepared by electrochemical polishing of a piece of thin wire. The tip is cooled to 12–80 K by being kept in thermal contact with a helium

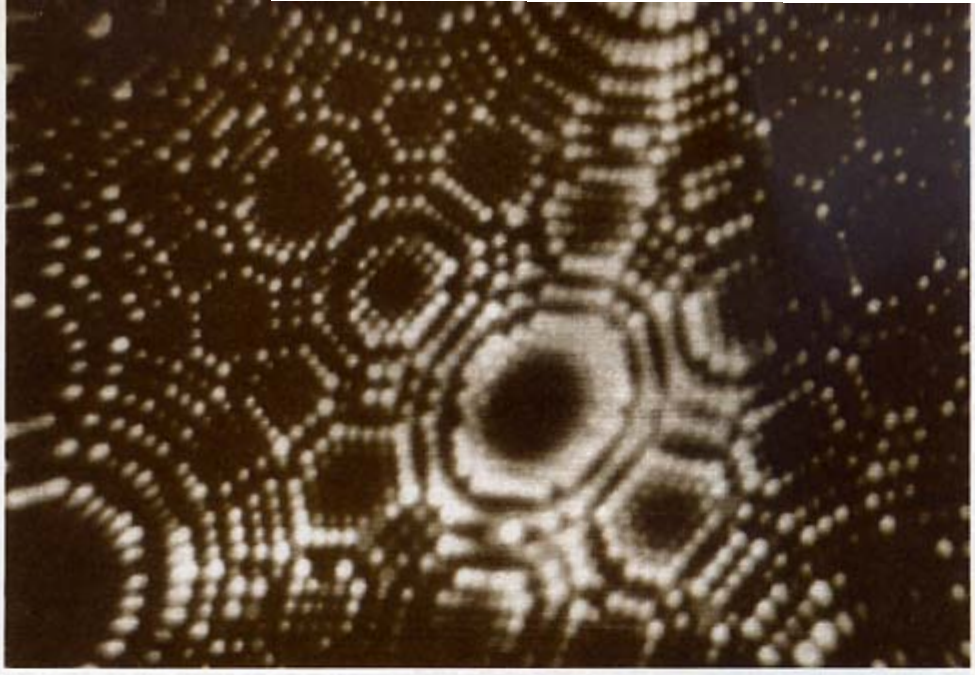

a

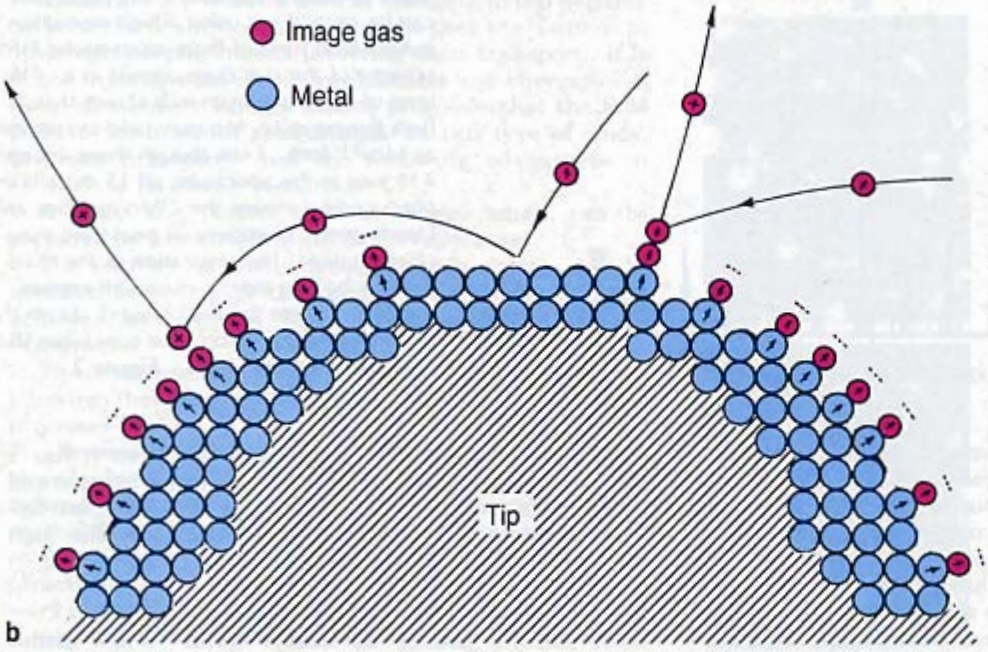

b

Imaging atoms by field ion microscopy. **a:** Field ion microscope image showing the (012) region of a nearly hemispherical Ir tip. Helium is the image gas. The tip is a stack of nearly circular atomic layers of different sizes. Each of the ring-like images is an atomic layer. At different orientations, there are small facets, some of which are atomically resolved. The variation in image intensity at the central (012) facet reflects field variation, which arises from an electronic smoothing effect at the atomic step. **b:** Schematic showing how an image is produced in the FIM. The emitter surface is first processed by field evaporation. In a field of a few volts per angstrom at low temperature, each apex site of the emitter atoms in the more protruding positions is field-adsorbed with an image-gas atom. The image-gas atoms, which are attracted to the emitter surface by a polarization force, hop around the surface and are field-ionized when they pass through the ionization zone (dashed line). Once ionized, they are accelerated to the screen to form a field ion image of the surface. **Figure 1**

refrigerator or cryogenic bath. The image chamber is filled with a gas, usually helium, to a pressure in the range of 10^{-5} torr. The dynamic gas supply mode is used so that a vacuum of at least 10^{-9} torr can be maintained in the flight tube section. For experiments involving single adsorbed atoms, the background pressure of the imaging chamber must be below 10^{-11} torr, and the purity of the image gas has to be very high to avoid surface contamination.

A field ion image is formed by field ionization of image gas atoms that lie above surface atoms occupying the more protruding sites. Field ionization of helium requires a positive field of about 4.5 V/Å. A field emitter prepared by electrochemical polishing usually has a rough surface with many tiny projections, or asperities. Such a surface is neither good for forming a high-resolution image of near-uniform magnification by radial projection of field ions nor good as a site for a surface physics experiment. (Some of the asperities may have single-atom sharpness and therefore may be suited for use in a scanning tunneling microscope.) Fortunately, when a positive voltage is applied to the tip and then gradually raised, adsorbed atoms and lattice atoms in the more protruding sites will desorb or evaporate. This "field evaporation" is a self-regulating process that eventually produces an atomically smooth emitter surface. The critical field needed for low-temperature field evaporation varies with the material. It ranges from less than 0.5 V/Å for alkali metals to about 5.7 V/Å for tungsten.

If the FIM is to yield a good image of a material, the critical field has to be greater than the image field. The required image field itself depends on the image gas. The best field ion images are obtained with neon and helium at fields of about 3.7 V/Å and 4.5 V/Å, respectively. Figure 1a shows a helium field ion image of an iridium field emitter surface, and figure 1b illustrates the physical processes involved in the formation of the image. The field ion image is a stereographic projection of the nearly hemispherical tip surface.

Figure 2a illustrates the chemical analysis aspect of the microscope. Using a gimbal system, one can adjust the

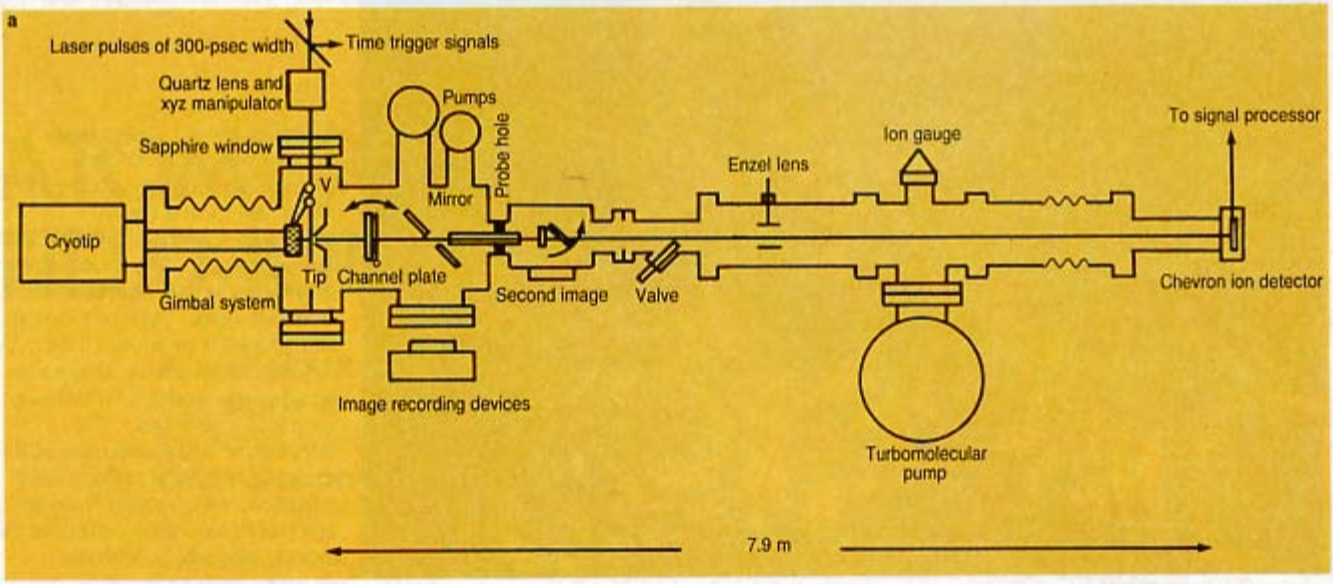

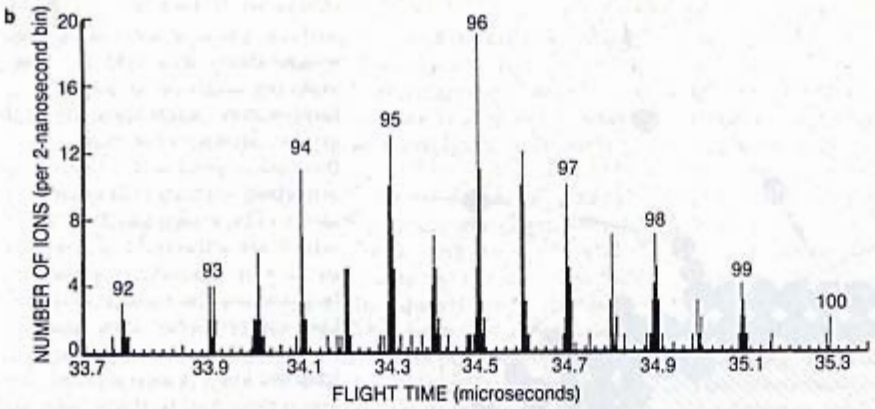

Mass spectroscopy and energy analyses can be carried out using a high-resolution pulsed-laser time-of-flight atom-probe FIM scheme of the sort diagrammed in **a**. The time-of-flight spectrum in **b** shows that at high temperature, Mo may field-evaporate as Mo_2^{2+} ions. Even though there are only 438 ions in this spectrum, all 15 mass lines produced by mixing the 7 Mo isotopes are clearly seen. Numbers on peaks are mass–charge ratios. The separation of the mass lines by half an atomic mass unit implies that the ions are doubly charged. From the abundance distribution, one concludes that there are few Mo^+ ions. **Figure 2**

orientation of the tip until the images of the atoms one intends to analyze fall into the probe hole. One then slowly pulse-field-evaporates emitter surface atoms using either nanosecond high-voltage pulses or laser pulses of subnanosecond width. Only ions produced by atoms whose images fall into the probe hole can go through the hole and be detected. One can derive both the mass-to-charge ratios and the kinetic energy distributions of the evaporated ions from their flight times. Because the high-voltage-pulse-evaporated ions have a large kinetic energy spread, one can often use, for example, a 163° electrostatic lens with flight-time focusing to improve the mass resolution. Such focusing systems are especially convenient for atomic-scale chemical analyses of metals and alloys. In my own laboratory we use a system of this sort for the atomic-layer-by-atomic-layer composition analysis of surfaces in the study of alloy segregations.

One can also operate the microscope with laser pulses that do not induce a large ion energy spread, thus greatly improving the resolution of the system and making it possible to analyze the energetics of surface atoms. In addition, one can analyze semiconductors and insulators without having to transmit electric pulses through the slender tip shank. We use a high-resolution pulsed-laser time-of-flight atom-probe FIM for many different studies: measurement of ion energy distributions in field evaporation and of site-specific binding energies of surface atoms; studies of ion cluster formation, field evaporation and field dissociation; chemical analyses of nonconducting materials; and so on. This microscope is a simple linear instrument, yet after an elaborate calibration it has a resolution and an accuracy of 1–2 parts in 10^5 in mass and energy analyses—a rarity for a time-of-flight spectrometer. Reference 4 discusses the reasons for this high resolution and the care in design needed to achieve it.

Dynamics of solid surfaces

Solid surfaces are by no means static. While lattice vibrations are familiar to all physicists, few know that even atoms of refractory metals can move on a metal surface quite freely at or below room temperature.[5] At higher temperatures atoms in the near-surface layers will start to move rapidly well before the melting point is reached.

Surface atoms can move either individually or collectively. Atoms are more likely to move collectively in structural phase transitions. Processes more likely to involve diffusion of single atoms or small atomic clusters include changes in shape of a solid, epitaxial growth of thin films, crystal growth, island formation from condensed atoms, some surface reconstructions, surface-enhanced chemical reactions, adsorption and desorption. In macroscopic studies of these phenomena, one tends to describe atom transport processes with the broad term "surface diffusion." But even in the simple case of crystal shape change, atoms first dissociate from their respective sites, then move on terraces, go up or down lattice steps and finally settle into new sites elsewhere. In other words, even a simple macroscopic phenomenon involves a series of "elementary atomic processes."

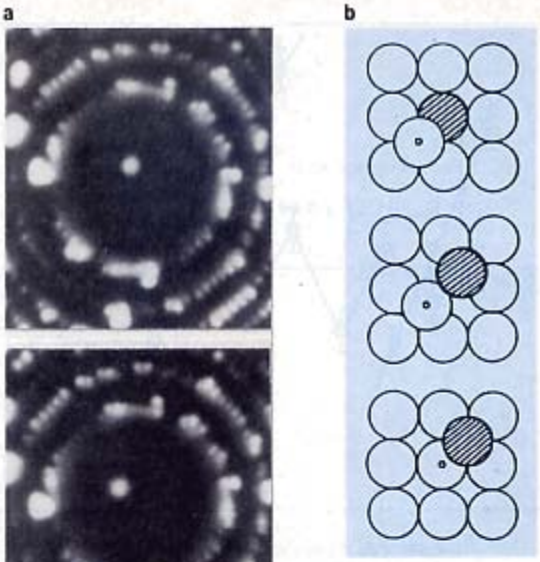

Random walk diffusion. **a:** Field ion images showing random walk diffusion of an Ir adatom on an Ir (001) surface. The dot near the center of each photograph is the image of the Ir adatom. The atomic structure of the substrate is revealed when the facet is reduced in size (bottom). **b:** Mapping the direction of the jump and the displacement of the adatom from successive images shows that the adatom moves in the diagonal direction of the square unit cell by concerted motion with a substrate atom. **Figure 3**

Unless one can study each of these elementary atomic processes individually, one cannot possibly understand the dynamics of the macroscopic phenomenon in terms of theories derived from first principles. Elementary atomic processes are universally used to understand the dynamical behavior of surfaces, and of course they are common to other surface phenomena involving atom transport. It is in the investigation of the mechanisms and energetics of these elementary surface atomic processes that the FIM finds its most useful applications. In this type of study, field ion microscopy has the following advantages in addition to its atomic resolution:

▷ A clean and perfect surface, though small, can be prepared by low-temperature field evaporation.

▷ The number of atoms deposited on a surface can be specified according to the needs of the study and then achieved by repeated deposition and controlled field evaporation.

▷ The temperature of the sample can be varied, thus allowing the quantitative study of thermally activated processes.

Several elementary atomic processes on surfaces have already been studied in detail with the FIM: surface diffusion of single adsorbed atoms (adatoms) and small atomic clusters, adatom–adatom interactions, site-specific atom–substrate interactions and adatom–lattice atom interactions. I will describe here only some of the recent work in this area, but first it is worthwhile to list a few significant results from earlier FIM studies:[5]

▷ The binding energy of an atom with the substrate is site-specific. For an atom whose coordination number is one-half that of a bulk atom, called a kink-site lattice atom, the measured binding energy agrees with the cohesive energy of the solid. For self-adsorption in other sites, the binding energy can vary from the latter value by as much as about 10%.

▷ For many systems, no direct chemical bond is formed between two adatoms. However, the adatoms can interact indirectly via the substrate by an electron hopping effect. Such interactions are weak, long range and oscillatory. Their strength is only on the order of 0.1 eV.

▷ The diffusion barrier height of an adsorbed atom depends on the atomic arrangement of the substrate. It is usually on the order of a few tenths of an electron volt, or about one-tenth the cohesive energy.

▷ A lattice step can be reflective or absorptive to a diffusing adatom. The height of reflective barriers is no greater than about 0.2 eV.

▷ No covalent bonds are formed between semiconductor adatoms such as silicon adatoms on a metal surface; that is, the metal surface makes the covalent bond nature of

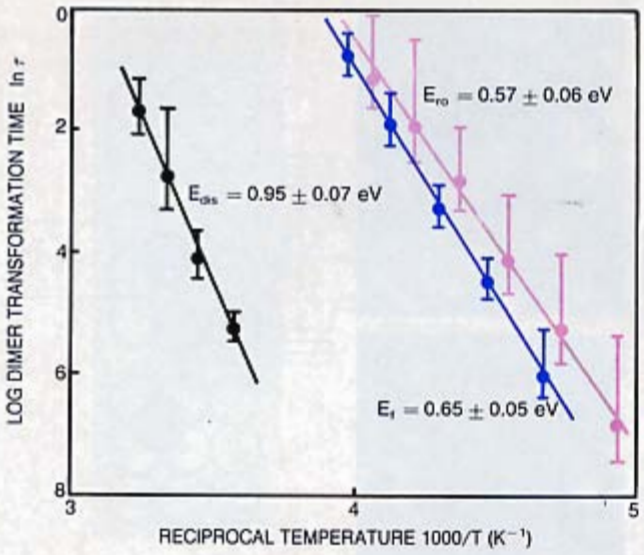

Dimer changes as a function of temperature. Upon heating, an Re adatom on the Ir (001) surface forms an Re–Ir dimer, which can reorient itself by 90° or dissociate. The barrier heights E_f, E_{ro} and E_{dis} for dimer formation, reorientation and dissociation, respectively, can be determined from the temperature dependences of their rates. **Figure 4**

the Si–Si interaction vanish.

I will elaborate on some of these results later.

Surface studies

In a typical surface diffusion study, one adatom is vapor-deposited onto one of the planar facets of the emitter surface. The adatom's displacement during a period of heating can be determined by direct comparison of its positions before and after the heating. Direct observations eliminate the need to extensively use models whose validity remains to be proven.

When there is no driving force, an adatom will perform a discrete, symmetric random lattice walk. Until last year,[6] the FIM was the only instrument that could observe directly the random walk of single adatoms and small atomic clusters and provide quantitative values of the diffusion parameters. The essential data in theories of random walk diffusion are the jump length distribution, the displacement distribution, the mean-square displacement and their temperature dependencies. The first quantity has to be derived by straightforward modeling, but the second two can be obtained directly by mapping the atomic positions with a PC-based image processing system. While the FIM's resolution is only about 2.5 Å, its accuracy in locating an atom's position is better than 0.5 Å. Figure 3a shows the random walk diffusion of an iridium adatom on an iridium (001) surface. It was known from earlier studies that an adatom performs discrete random hopping on the two-dimensional periodic lattice of the surface.

The barrier height and the atomic vibrational frequency factor are determined from the slope and intercept of an Arrhenius plot, which is a linear plot of the logarithm of the mean-square displacement per unit time versus the inverse temperature. The frequency factors are found to be consistently in the range of 10^{12}/sec to 10^{13}/sec for all the diffusion systems studied. The barrier height varies from less than 0.2 eV for diffusion on the smooth (111) surface of face-centered-cubic metals to over 1.5 eV for rough surfaces like the (111) surface of body-centered-cubic metals, but is specific to the chemical species and the atomic arrangement of the diffusion system. At low temperatures, atomic hopping is almost always confined to the nearest-neighbor distance.

An adatom that diffuses on a surface consisting of closely packed atomic rows separated by fairly deep surface channels, such as the W {112} and Pt and Ir {110} surfaces, can replace an atom in the channel wall.[7] A surprising recent FIM finding is that in self-diffusion on fcc surfaces such as the {001} surface of Pt or Ir, surface atoms move by an atomic replacement, or atomic exchange, mechanism.[8] For example, upon heating to over 240 K, an Ir adatom will replace a lattice atom while the two are in concerted motion, as figure 3b illustrates. This results in an apparent atomic jump in the diagonal direction of the square unit cell of the surface lattice. Although the displaced adatom is not the original one, the two are identical. Surfaces that can reconstruct favor atomic replacement self-diffusion. In fact, in the (1×1) to (1×2) reconstruction of the Pt and Ir {110} surfaces, simultaneous replacement diffusion of small ⟨110⟩ rows of atoms can occur.

In a two-element system, the atomic replacement mechanism produces alloying at an atomic site followed by self-diffusion of the displaced substrate atom rather than diffusion of the foreign atom. A particularly interesting system[9] is Re–Ir {001}. Upon heating to above 220 K, the image of a vapor-deposited Re adatom is replaced with the image of a dimer, presumably an Re–Ir pair. The dimer can change its orientation by 90° when the temperature reaches around 200–260 K. Upon heating to over 280 K, the dimer dissociates, the Re atom is incorporated into the substrate lattice, and the replaced Ir atom diffuses elsewhere. All these atomic steps are revealed in the FIM images when the observation is combined with low-temperature field evaporation. More important, one can study the energetics of these atomic processes by measuring the rates of the atomic steps, as shown in figure 4. Alloying at single atomic sites on the top surface layer, as occurs in the Re–Ir system, should be a valuable process for creating a thermally stable atomic feature through atomic manipulation.

Measured binding energies vs cohesive energies

Metal	Measured binding energy E_b (eV)	Cohesive energy E_c (eV)	Difference (eV)
Fe	4.50 ± 0.16	4.32	$+0.18 \pm 0.16$
Co	4.34 ± 0.08	4.41	-0.07 ± 0.08
Ni	4.35 ± 0.04	4.46	-0.11 ± 0.04
Rh	5.74 ± 0.22	5.78	$+0.04 \pm 0.22$
W	9.00 ± 0.49	8.90	$+0.10 \pm 0.49$
Pt	5.62 ± 0.12	5.84	-0.22 ± 0.12
			(Average = -0.01 ± 0.24)
Co in Pt_3Co	4.98 ± 0.16	Unknown	
Pt in Pt_3Co	5.53 ± 0.17	Unknown	

Site-specific binding energy

The cohesive energies of solids are usually derived by thermodynamic methods, and reliable data are available. Two interesting questions are how much energy is needed to remove an atom from a surface and how this energy depends on the atomic environment of the atom or the site of the atom. In the 1930s, J. B. Taylor and Irving Langmuir

developed a thermal desorption method to measure the desorption energy of adsorbed species.[10] This method has now been developed into a popular temperature-programmed desorption method for measuring the binding energies in different adsorption states of chemisorbed species. However, when the temperature is raised, atoms and molecules can diffuse on the surface before they are desorbed. Neither the mechanisms of desorption nor the sites where desorption occurs are known. Taylor and Langmuir rightfully called these energies thermal desorption energies, not binding energies. Here I will describe new methods, by which one can determine site-specific binding energies of some surface atoms.

A field ion microscopy method can be used to measure the kinetic energy distribution of low-temperature field-evaporated ions.[11] In atom-probe field ion microscopy, atoms can be field-evaporated at low temperature directly from their sites. It can be shown by consideration of a Born–Haber energy cycle that the critical ion energy deficit is directly related to the binding energy of these atoms. (The critical ion energy deficit is the energy deficiency of the most energetic ions of an ion species relative to the acceleration energy neV, where n is the charge state of the ions and V is the tip voltage.) By measuring very accurately the critical ion energy deficit of low-temperature field-evaporated ions using the high-resolution pulsed-laser time-of-flight atom-probe FIM shown in figure 2, one thus can derive the site-specific binding energies of these surface atoms.

In low-temperature field evaporation of lattice atoms, desorption is mostly from kink sites at the lattice steps. When the probe hole is aimed at a lattice step, the binding energy measured is that of kink-site atoms. The table on page 28 lists the kink-site binding energies E_k so obtained for several metals and alloys. Because kink sites provide an identical atomic environment from which one can remove nearly all the atoms in a solid, all such removals require the same energy. From this simple argument, the binding energy of kink-site atoms should be equal to the cohesive energy E_c, although there have been no experimental data to substantiate this argument. As can be seen from the table, within the approximately 0.2-eV accuracy of the measurement, all the data derived for metals agree with their cohesive energies.

One may worry about how the field is going to change the measured binding energy. However, the fact that the measured values agree with theoretically expected values to within 0.2 eV indicates that this method is at least that accurate in binding energy measurements. This method can of course be applied to measure the binding energy of atoms at other sites such as the adsorption site. Because of a few practical difficulties, such measurements have not yet been made.

The binding energy E_b of adatoms in self-adsorption can be more easily determined from a measurement of the thermal dissociation rate. It can be shown that $E_b = E_c + E_d - E_{dis}$, where E_d is the activation energy for adatom diffusion and E_{dis} is the dissociation energy for a kink-site atom to move to a terrace site. E_{dis} can be determined from an Arrhenius-like plot of the dissociation time of a surface layer as a function of temperature in the thermal blunting process of a field ion emitter. For Ir on the Ir {001} surface, E_{dis} is[12] 1.40 ± 0.08 eV. The binding energy of an Ir adatom on the Ir {001} surface is therefore $E_c - E_b = E_{dis} - E_d$, 0.56 ± 0.08 eV smaller than that of kink-site atoms.

Oscillatory surface segregation

The atomic structure and the distribution of constituent atoms provide essential information about a solid surface, because they determine its physical and chemical properties. While many macroscopic and microscopic techniques are now available for determining the atomic arrangements in the top and near-surface layers, the same cannot be said about the composition variation. Even when a technique is surface sensitive, to reach into the near-surface layers one invariably relies on ion sputtering to remove the top layer. This not only creates lattice defects but also introduces atomic mixing between surface layers.

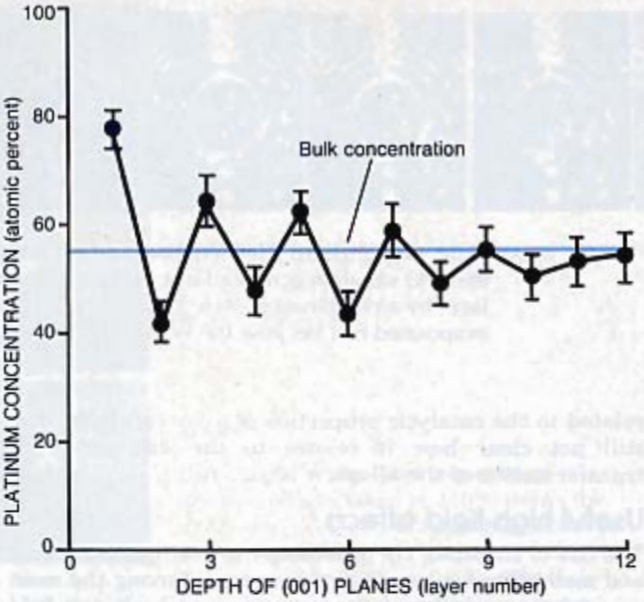

Composition oscillation. When a Pt–Rh alloy is thermally annealed to equilibrate the distribution of Pt and Rh atoms in the near-surface layers, the composition of those layers is found to oscillate with depth. **Figure 5**

So far only a few composition analysis studies have achieved true depth resolution of atomic layers. An indirect method used a theoretical model to analyze spot intensities in low-energy electron diffraction. This technique found an atomic-layer-by-atomic-layer oscillatory variation in the composition of the top three atomic layers of Pt–Ni alloy surfaces.[13] Pt–Rh alloys showed similar behavior in an earlier direct composition analysis with an atom-probe FIM.[14] In that study, we annealed an alloy tip to high temperature to thermally equilibrate the distribution of alloy components in the near-surface layers and then quenched the tip. We aimed the probe hole at the edge of the top surface layer and carried out slow pulsed-field evaporation. As we gradually field-evaporated and analyzed the edge atoms one by one, and as the edge of the layer gradually receded, we adjusted the orientation of the tip so that the probe hole was always aimed at the layer edge. When the top layer was completely field-evaporated, we analyzed the second layer. With this method, one can analyze the absolute composition of the near-surface layers one by one.

Studies with the atom-probe FIM have already found long-range oscillation in alloy composition. A recent novel finding is that in Pt–Rh alloys, not only is Pt enriched at the top surface layer, but the composition oscillates toward the bulk value with a wavelength of two atomic layers, as shown in figure 5. If the alloy contains a trace of sulfur, sulfur atoms segregate to the surface to form an overlayer, and the top alloy layer becomes enriched with Rh. This surface segregation behavior is intimately

Field evaporation. This sequence of field ion images shows the well-controlled nature of field evaporation and the field variation across a facet. Seven tungsten adatoms were field-evaporated one by one from a W (110) facet by a combination of dc bias and high-voltage pulses. Adatoms closer to the plane edge are field-evaporated first because the field is higher there. **Figure 6**

related to the catalytic properties of alloy catalysts; it is still not clear how it relates to the disorder–order transformation of the alloys.[15]

Useful high-field effects

The use of scanning tip microscopy to manipulate atoms and molecules is a recent development. Among the most promising methods are ones using high-electric-field effects such as field evaporation and field-gradient-induced surface diffusion. Creating an atomic feature on a solid surface may involve three tasks:

- ▷ movement of an atom from one location on the surface to another
- ▷ deposition of an atom on a surface, preferably at the intended location
- ▷ removal of prespecified atoms from the surface.

For these tasks, one may use the intrinsic interaction between the surface atom one intends to move and the atoms of the probing tip.[16] This is most convenient for moving physisorbed atoms. For moving more strongly bonded, chemisorbed atoms, one can use two methods. One method is based on field evaporation.[16] First, one places the tip above the surface. One then applies an electric pulse of appropriate polarity to the sample, causing the desired atom to be emitted from the sample surface to the tip surface. One moves the tip to the new location and applies a pulse to the tip, transferring the atom back to the sample. In the second method, one first moves the tip to a position near the adatom in question. Applyping a voltage bias or pulse of appropriate polarity to the sample causes the adatom to move from the original location to a spot directly below the tip.[17] This motion is produced by a directional diffusion induced by a field gradient.

Field evaporation is essential in field ion microscopy for processing the emitter surface, for removing atoms from the surface layers to reach inside the bulk and for chemically analyzing the surface by mass spectrometry. The field strength controls the field evaporation well. The field near a lattice step of a facet is higher than that near the center. When the tip voltage is raised, adatoms closer to the step are field-evaporated first, one at a time. Figure 6 shows how seven tungsten atoms vapor-deposited on the (110) facet of a tungsten field emitter were field-evaporated one at a time using high-voltage pulses added to a dc bias.

The critical field for evaporation to occur and the charge state of ions emitted can be calculated from simple theoretical models and verified experimentally.[4] Two simple models, the image hump model and the charge exchange model, predict that soft metals like Al, Cu, Pd, Ag, Au and Pb will field-evaporate as singly charged positive ions. Most metals—such as Be, Ni, Co, Fe, Ru, Rh and Pt—and semiconductors—such as Si and Ge—are predicted to field-evaporate as 2+ ions. Refractory metals—such as Ta, W and Re—should field-evaporate as 3+ ions. These charge states agree very well with atom-probe mass analyses of low-temperature field-evaporated ions. The critical fields calculated from the two models agree with each other very well. They also agree with experimental values to within 15%.

Field evaporation in the double-electrode geometry of the scanning tunneling microscope is slightly different from that in the field ion microscope.[18,19] In the STM, if the tip-to-sample distance is within the range of atomic interaction, direct transfer of atoms can occur between the tip and the sample. This transfer is not unidirectional but depends on the probabilities given by the Boltzmann factors. With an applied field, the atom transfer becomes directional. The atom is probably only partially charged during the transfer, but the question of which is the preferred direction remains unanswered.

If, however, the separation is large enough that there is no significant overlap of the wavefunctions from the tip side and the sample side, then theoretical models used in field ion microscopy can be applied to the STM with only minor modifications. First, one must account for the fact that both the surface atom to be field-evaporated and the ion formed can interact with the sample as well as the tip. Second, one must consider the possibility that atoms can field-evaporate in a negative field as negative ions. Third, one should consider how the critical fields depend on the tip-to-sample separation. My coworkers and I have done such calculations recently for gold and silicon. To our surprise, the critical fields for forming 2− ions are the lowest among the charge states considered, and at a tip-to-sample distance typical of the STM the critical fields are only about one-third of those seen in more usual configurations of the FIM.[19] This result is consistent with STM observations, although no experimental evidence exists of field evaporation as 2− ions for these elements in the STM.

One method of moving adsorbed atoms in a controlled manner using the STM is based on the observation that when a voltage bias or pulse of appropriate polarity is applied to the sample, Cs adatoms on a GaAs surface tend to move from the neighborhood of the tip to the spot directly below the tip.[17] This motion is produced by a field-gradient-induced surface diffusion found and studied earlier in the FIM. In the FIM, when the random walk of an adatom is carried out on a field-emitter facet with the image voltage applied, the adatom drifts directly from the central region to the edge of the facet,[20] as can be seen in figure 7. In the absence of an applied tip voltage, the potential energy of the adatom–surface interaction is horizontal and periodic, and the adatom performs a symmetric random walk. When a voltage is applied to the tip, the field at the central region becomes lower than that near the edge, where the polarization binding is larger. When the polarization energy of the adatom is included,

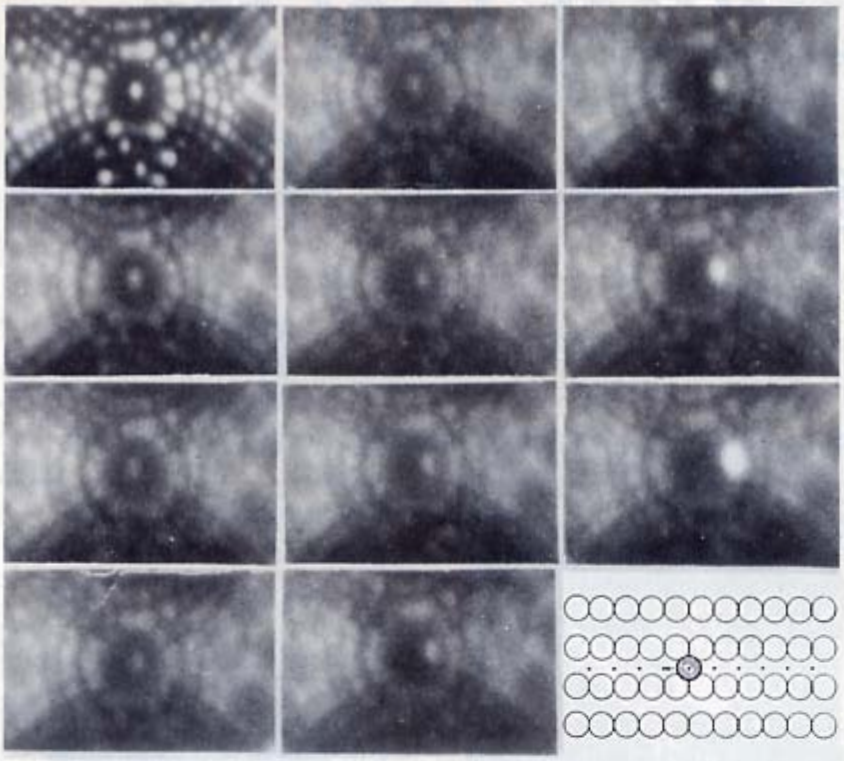

Directional walk. This sequence of field-ion images taken at 270 K shows the directional walk of one tungsten adatom on a W (112) surface. The sequence order is first top to bottom, then left to right. Starting from the fifth image, the adatom jumps toward the plane edge one step at a time. Variation of the image brightness of the adatom reflects variation of the field. The schematic diagram at the lower right maps the adatom's movement. **Figure 7**

the surface potential becomes inclined. Thus the adatom will jump preferentially toward the plane edge.

One can measure the field gradient from the critical fields of desorbing adatoms at different positions. By also measuring both the drift velocity as a function of the applied field and the mean-square displacement per unit time in zero applied field, one can determine the surface-induced dipole moment and the effective polarizability of the adatom from the intercept and slope of a graph known as a τ plot.[20] These parameters for tungsten adatoms on the tungsten (110) surface have been measured to be 1.0 debye and 14 Å^3, respectively, although the accuracy of the experiment is still limited. This field-gradient-induced directional diffusion of adatoms explains the STM observation of Cs adatoms moving on a GaAs surface. The field gradient in that case arises from the geometrical asymmetry of the tip–sample configuration. The field is highest at the spot just below the tip. Based on a simple method, it is estimated[17] that the polarizability of Cs atoms on the GaAs (111) surface is about 50 Å^3, a reasonable value for the large Cs atom.

There are many other effects of the electric field that may be useful for atomic manipulations. For example, by using temperature- and field-gradient-induced surface diffusion, one can process the tip to single-atom sharpness for use as an electron source in the field emission mode.[21] In the field ion emission mode, the tip can be maintained at the same sharpness while emitting ions at a rate of 10^6–10^7/sec. The development of arrays of such sharp tips for image display panels is generating great interest.[22] Discussion of these and other applications is, however, beyond the scope of this article.

References

1. E. W. Müller, Z. Phys. **131**, 136 (1951).
2. E. W. Müller, J. A. Panitz, S. B. McLane Jr, Rev. Sci. Instrum. **39**, 83 (1968).
3. M. K. Miller, G. D. W. Smith, *Atom-Probe Microanalysis: Principles and Applications to Materials Problems*, Mater. Res. Soc., Pittsburgh (1989). T. Sakurai, S. Sakai, H. Pickering, *Atom-Probe Field Ion Microscopy and Its Applications*, Academic, New York (1989). J. Orloff, Sci. Am., October 1991, p. 96. A. Cerezo, T. J. Godfrey, G. D. W. Smith, Rev. Sci. Instrum. **59**, 862 (1988).
4. T. T. Tsong, *Atom-Probe Field Ion Microscopy*, Cambridge U. P., New York (1990). T. T. Tsong, Y. Liou, S. B. McLane, Rev. Sci. Instrum. **55**, 1246 (1984).
5. G. Ehrlich, K. Stolz, Annu. Rev. Phys. Chem. **31**, 603 (1980). T. T. Tsong, Rep. Prog. Phys. **51**, 759 (1988).
6. For a quantitative STM study of single-atom diffusion, see E. Ganz, S. K. Theiss, I. S. Huang, J. A. Golovchenko, Phys. Rev. Lett. **68**, 1567 (1992).
7. D. W. Bassett, P. R. Weber, Surf. Sci. **70**, 520 (1978). J. D. Wrigley, G. Ehrlich, Phys. Rev. Lett. **44**, 661 (1980).
8. G. L. Kellogg, P. J. Feibelman, Phys. Rev. Lett. **64**, 3143 (1990). L. Chen, T. T. Tsong, Phys. Rev. Lett. **64**, 3147 (1990).
9. T. T. Tsong, C. L. Chen, Nature **355**, 328 (1992).
10. J. T. Yates, Methods Exp. Phys. **22**, 425 (1985).
11. J. Liu, C. W. Wu, T. T. Tsong, Phys. Rev. B **45**, 3659 (1992).
12. C. L. Chen, L. H. Zhang, Z. W. Yu, T. T. Tsong, Phys. Rev. B **46**, 7803 (1992).
13. Y. Gauthier, R. Baudoing, M. Lundberg, J. Rundgren, Phys. Rev. B **35**, 7867 (1987), and refs. therein.
14. M. Ahmad, T. T. Tsong, J. Chem Phys. **83**, 388 (1985). D. M. Ren, J. H. Qin, J. B. Wang, T. T. Tsong, Phys. Rev. B **47**, 3944 (1993).
15. J. Tersoff, Phys. Rev. B **42**, 10965 (1990).
16. D. M. Eigler, E. K. Sweizer, Nature **344**, 524 (1990).
17. L. J. Whitman, J. A. Stroscio, R. A. Dragoset, R. J. Celotta, Science **251**, 1206 (1991).
18. H. J. Mamin, P. H. Guethner, D. Rugar, Phys. Rev. Lett. **65**, 2418 (1990). N. Lang, Phys. Rev. B **45**, 13599 (1992).
19. N. M. Miskovsky, C. M. Wei, T. T. Tsong, Phys. Rev. B **46**, 2640 (1992); Phys. Rev. Lett. **69**, 2427 (1992).
20. T. T. Tsong, G. L. Kellogg, Phys. Rev. B **12**, 1343 (1975). S. C. Wang, T. T. Tsong, Phys. Rev. B **26**, 6470 (1982).
21. V.-T. Binh, S. T. Purcell, N. Garcia, J. Doglioni, Phys. Rev. Lett. **69**, 2527 (1992).
22. I. Brodie, C. A. Spindt, Adv. Electron. Electron Phys. **83**, 2 (1992). ■